

## Interaction between Surface Hydroxyl Groups and Adsorbed Molecules

### III. The Nature of the Adsorbate-Hydroxyl Interaction\*†

J. A. CUSUMANO

*Corporate Research Laboratories, Esso Research and Engineering Company, P.O. Box 45,  
Linden, New Jersey 07036*

AND

M. J. D. LOW

*Department of Chemistry, New York University, New York, New York 10453*

Received February 25, 1971

An analysis of the possible modes of interaction between benzenes and substituted benzene with surface hydroxyl groups pointed to the occurrence of charge transfer processes. Consequently, Mulliken-Puranik charge-transfer theory was applied to the systems. For a  $\pi$ -OH interaction, the model involves the formation of an asymmetrically bonded surface complex, an electron entering the antibonding orbital of the surface hydroxyl, interaction occurring between that orbital and the aromatic  $\pi$ -system along one of the C-C lengths. The charge-transfer theory led to relations between the shift of the hydroxyl absorption frequency,  $\Delta\nu_{\text{OH}}$ , and the ionization potential of the adsorbate, and also between  $\Delta\nu_{\text{OH}}$  and the change in the hydroxyl absorption intensity, brought about by the adsorbate-OH interaction. An analysis of adsorption data showed that the charge-transfer theory was quite successful in explaining the interactions of surface hydroxyls not only with aromatics but with a large variety of other adsorbents.

#### INTRODUCTION

We have studied the adsorption of a variety of substances on porous glass in order to gain information about the nature of the interaction between aromatic molecules and surface hydroxyl groups. The initial studies used benzene as a model adsorbate. The thermodynamic and statistical mechanical aspects of the benzene-porous glass system, deduced from gravimetric measurements, were described in Part I (1); complementary data obtained by infrared spectroscopic measurements are

described in Part II (2). Such studies were then extended to other adsorbates mainly in order to obtain infrared spectroscopic data. The latter, as well as literature data, are used in the present Part III to develop a model concerning the nature of the adsorbate-OH interactions.

#### EXPERIMENTAL

Experimental procedures were described earlier (1, 2). Adsorbates were purified in a manner similar to that used for benzene (1, 2). The shifts in the stretching fundamental of free surface OH groups,  $\Delta\nu_{\text{OH}}$ , were measured at a surface coverage  $\theta = 0.5$ , and are based on the fundamental vibrational frequency of free Si-OH groups as a reference point, although it should be clear that

\* Part I, Ref. (1); part II, Ref. (2).

† Presented at the *North American Meet. Catal. Soc. Ist.*, and abstracted, Atlantic City, New Jersey, February 20, 1969.

TABLE 1  
POTENTIAL CORRELATIVE PARAMETERS FOR THE ADSORPTION OF VARIOUS AROMATIC MOLECULES  
ON POROUS VYCOR GLASS

| No. <sup>a</sup> | Adsorbate  | $\Delta\nu_{\text{OH}}$<br>( $\text{cm}^{-1}$ ) | $(\Delta\nu_{\text{OH}}/\nu_0)^{-1/2b}$ | $I_D$ (eV) <sup>c</sup> | $\mu$<br>(Debyes) <sup>d</sup> | $(\epsilon + 1)/(2\epsilon + 1)^d$ | $\sigma_p^e$ | $\sigma_m^e$ | Ref.<br>for<br>$\Delta\nu_{\text{OH}}$ |
|------------------|--|---|---|-------------------------|--------------------------------|------------------------------------|--------------|--------------|--|
| 26               | $\phi$ -H  | 127   | 5.44                                    | 9.25                    | 0                              | 0.231                              | —            | —            | —                                      |
| 31               | $\phi$ -F  | 59  | 8.00                                    | 9.19                    | 1.59                           | 0.391                              | +0.062       | +0.337       | —                                      |
| 37               | $\phi$ -OCH <sub>3</sub>                           | {350<br>150}                                    | {3.27<br>5.00}                          | 8.20                    | 1.35                           | 0.345                              | -0.268       | +0.115       | (27)                                   |
| 32               | $\phi$ -CF <sub>3</sub>                            | 33  | 10.70                                   | 9.68                    | 2.56                           | —                                  | +0.551       | +0.415       | (27)                                   |
| 27               | $\phi$ -CH <sub>3</sub>                            | 145   | 5.10                                    | 8.82                    | 0.37                           | 0.234                              | -0.170       | -0.069       | —                                      |
| 28               | $\phi$ -C(CH <sub>3</sub> ) <sub>3</sub>           | 150   | 5.00                                    | 8.69                    | 0.70                           | 0.330                              | -0.197       | -0.120       | —                                      |
| 33               | $\phi$ -OH   | 350   | 3.27                                    | 8.50                    | —                              | —                                  | -0.357       | -0.002       | (7)                                    |
| 6                | $\phi$ -NH <sub>2</sub>                            | {550<br>150}                                    | {2.61<br>3.00}                          | 7.70                    | 1.48                           | 0.401                              | -0.660       | -0.161       | (26)                                   |
| 35               | $\phi$ -NO <sub>2</sub>                            | 140   | 5.18                                    | 10.1                    | 4.23                           | —                                  | +0.778       | +0.710       | (26)                                   |
| 29               | <i>p</i> - $\phi$ -(CH <sub>3</sub> ) <sub>2</sub> | 160   | 4.85                                    | 8.45                    | —                              | 0.230                              | —            | —            | —                                      |
| 30               | Sym- $\phi$ -(CH <sub>3</sub> ) <sub>2</sub>       | 166   | 4.74                                    | 8.39                    | 0                              | —                                  | —            | —            | —                                      |
| 40               | Cyclohexane  | 27  | 11.80                                   | 9.88                    | 0                              | 0.203                              | —            | —            | —                                      |
| 36               | $\phi$ -CHO  | 290   | 3.60                                    | 9.51                    | —                              | —                                  | +0.216       | +0.355       | —                                      |

<sup>a</sup> These numbers refer to the data points of Fig. 8.

<sup>b</sup>  $\nu_0$  can vary by a few wavenumbers, depending on the degree and severity of outgassing of the adsorbate. The value of  $\nu_0$  was consequently chosen as  $3750 \text{ cm}^{-1}$ .  $\Delta\nu_{\text{OH}}$  values refer to a surface coverage of  $\theta = 0.5$ .

<sup>c</sup> Data from Ref. (29).

<sup>d</sup> Data from Ref. (38).

<sup>e</sup> Data from Ref. (39).

at this surface coverage interaction is established with only B-OH groups [see Fig. 3 in Ref. (2)].  $\Delta\nu_{\text{OH}}$  values for a series of adsorbates are listed in Table 1. Other data taken from the literature are listed in Table 2.

In order to aid the discussion, some mathematical treatments are outlined in the Appendix.

## RESULTS AND DISCUSSION

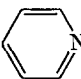
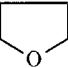
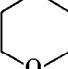
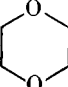
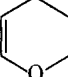
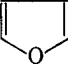
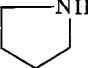
It is well known that the hydroxyls on solid surfaces are frequently "perturbed" when adsorption occurs. The OH infrared band shifts, broadens, and changes in intensity, indicating that some interaction has occurred with the adsorbed material, and such effects have frequently been attributed to hydrogen bonding between the adsorbate and surface hydroxyls (3-7). Many of such effects are described in Little's monograph (7). There have, however, been few attempts to use such observations to derive a quantitative or even semiquantitative model

concerning the nature of the adsorbate-OH interaction. Even a simple theory should be able to explain (a) the shift in the OH band to lower frequencies with increasing interaction, and (b) the increase in the OH absorption with hydrogen bond formation, and this will be attempted.

### Classical Theories

As  $\Delta\nu_{\text{OH}}$  was directly related to the surface interaction and the surface-bond energy, it was pertinent to see how  $\Delta\nu_{\text{OH}}$  was related to physically measurable parameters which, in turn, could be considered in terms of the standard theories of the hydrogen bond. However, attempts to apply the classical theories to the present data showed that the models used could not explain the surface interactions adequately. For example, Fig. 1 shows  $\Delta\nu_{\text{OH}}$  as a function of the molecular dipole moment of the adsorbate. There is little correlation between the parameters so that the dipole theory (3) appears to be inadequate. However, this is not surprising,

TABLE 2  
CHARGE-TRANSFER DATA FOR VARIOUS ORGANIC ADSORBATES

| No. <sup>a</sup> | Compound  | $\Delta\nu_{\text{OH}}$ (cm <sup>-1</sup> ) | $I_D$ (eV) <sup>b</sup> | $(\Delta\nu_{\text{OH}}/\nu_0)^{-1/2c}$ | Ref. |
|------------------|---|---|-------------------------|---|------|
| 1                | NH <sub>3</sub>   | 675   | 10.16                   | 2.36                                    | (33) |
| 2                |    | 765   | 9.70                    | 2.22                                    | (34) |
| 3                | (C <sub>2</sub> H <sub>5</sub> ) <sub>3</sub> N                                     | 975   | 7.50                    | 1.96                                    | (7)  |
| 4                | (CH <sub>3</sub> ) <sub>3</sub> N   | 990   | 7.80                    | 1.95                                    | (37) |
| 5                | (C <sub>2</sub> H <sub>5</sub> ) <sub>2</sub> N                                     | 990   | 8.01                    | 1.95                                    | (7)  |
| 6                | $\phi$ -NH <sub>2</sub>   | 550   | 7.70                    | 2.61                                    | (29) |
| 7                | (CH <sub>3</sub> ) <sub>2</sub> O   | 420   | 10.00                   | 3.00                                    | (7)  |
| 8                | (C <sub>2</sub> H <sub>5</sub> ) <sub>2</sub> O                                     | 445   | 9.53                    | 2.90                                    | (7)  |
| 9                | ( <i>n</i> -C <sub>3</sub> H <sub>7</sub> ) <sub>2</sub> O                          | 470   | 9.27                    | 2.82                                    | (7)  |
| 10               | SiCl <sub>4</sub>   | 25  | 11.6                    | 12.22                                   | (35) |
| 11               |    | 475   | 9.54                    | 2.81                                    | (7)  |
| 12               |    | 490   | 9.26                    | 2.76                                    | (7)  |
| 13               |    | 430   | 9.13                    | 2.96                                    | (7)  |
| 14               |   | 430   | 8.34                    | 2.96                                    | (7)  |
| 15               |  | 120   | 8.89                    | 5.45                                    | (7)  |
| 16               |  | 325   | 8.20                    | 3.40                                    | (7)  |
| 17               | CS <sub>2</sub>   | 60  | 10.40                   | 7.88                                    | (32) |
| 18               | <i>n</i> -C <sub>5</sub> H <sub>12</sub>  | 30  | 10.35                   | 11.29                                   | (7)  |
| 19               | <i>n</i> -C <sub>6</sub> H <sub>14</sub>  | 37  | 10.18                   | 10.06                                   | (7)  |
| 20               | <i>n</i> -C <sub>7</sub> H <sub>16</sub>  | 45  | 10.08                   | 9.20                                    | (7)  |
| 21               | CCl <sub>4</sub>  | 40  | 11.47                   | 9.68                                    | (7)  |
| 22               | CHCl <sub>3</sub>   | 48  | 11.42                   | 8.86                                    | (7)  |
| 23               | CH <sub>2</sub> Cl  | 72  | 11.35                   | 7.23                                    | (7)  |
| 24               | CH <sub>3</sub> Cl  | 106   | 11.28                   | 5.95                                    | (7)  |
| 25               | CH <sub>3</sub> I   | 125   | 9.54                    | 5.46                                    | (32) |
| 38               | CH <sub>3</sub> CHO   | 280   | 10.21                   | 3.66                                    | (32) |
| 39               | CH <sub>3</sub> NO <sub>2</sub>   | 160   | 11.08                   | 4.85                                    | (7)  |
| 41               | CH <sub>3</sub> COOC <sub>2</sub> H <sub>5</sub>                                    | 280   | 10.11                   | 3.66                                    | (7)  |
| 42               | CH <sub>3</sub> CN  | 220   | 12.22                   | 2.92                                    | (33) |
| 43               | SO <sub>2</sub>   | 115   | 12.34                   | 5.69                                    | (7)  |
| 44               | (CH <sub>3</sub> ) <sub>2</sub> CO  | 330   | 9.69                    | 3.36                                    | (7)  |

<sup>a</sup> These numbers refer to the data points of Fig. 8.

<sup>b</sup> Data from Ref. (29).

<sup>c</sup>  $\nu_0$  can vary by a few wavenumbers, depending on the degree of severity of outgassing of the adsorbent. The value of  $\nu_0$  was consequently taken as 3750 cm<sup>-1</sup>.  $\Delta\nu_{\text{OH}}$  values refer to a surface coverage of  $\theta = 0.5$ . Whenever adsorption data were insufficient, the value of  $\Delta\nu_{\text{OH}}$  was obtained by extrapolation, or estimated from the maximum  $\Delta\nu_{\text{OH}}$  observed for the particular compound and  $\Delta\nu_{\text{OH}} = f(\theta)$  for a similar compound for which data were available. In any case, for  $\Delta\nu_{\text{OH}} > 100$  cm<sup>-1</sup>, the error in  $\Delta\nu_{\text{OH}}$  is less than 10%.

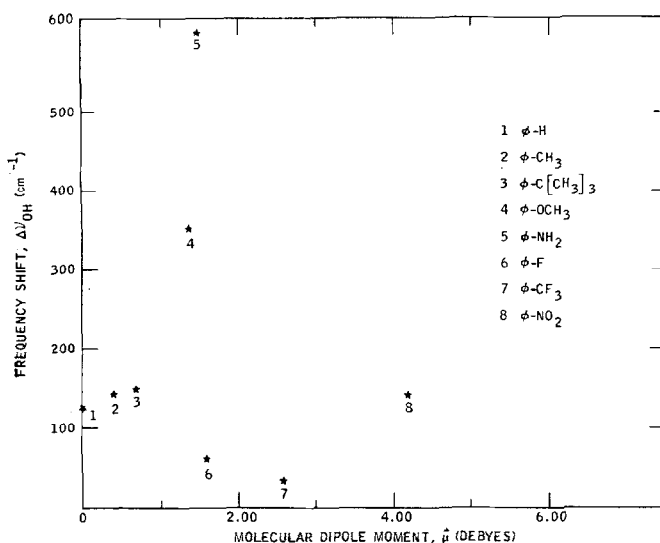


FIG. 1. Frequency shift of the hydroxyl absorption as function of the molecular dipole moment of various aromatic molecules, for adsorption on porous Vycor glass at room temperature at a surface coverage of  $\theta = 0.5$ .

because that theory considers dispersion forces as the prime mechanism for bond formation and neglects the electron delocalization effects which can be very important with  $\pi$ -electron systems.

Figure 2 shows  $\Delta\nu_{OH}$  plotted versus the Kirkwood functions  $(\epsilon - 1)/(2\epsilon + 1)$ ,  $\epsilon$  being the bulk dielectric constant of the adsorbate. The correlation is marginal, suggesting the Kirkwood-Bauer-Magat (9, 10) theory to be inadequate. As Little has suggested (7), the KBM theory has been found to be inadequate in accounting for the effects produced by polar adsorbates probably because values for macroscopic dielectric properties cannot be applied successfully to the immediate molecular environment of adsorbed species.

Another correlation uses the Hammett equation (11),

$$\log K/K_0 = \rho\sigma,$$

where  $\sigma$  (the substituent constant) is taken to be a measure of the ability of a substituent to alter the ring-electron density of benzenes. Figure 3 shows  $\Delta\nu_{OH}$  as a function of the parasubstituent constant  $\sigma_p$ . The available data appears to fall into two groups. It is interesting to note that, as mentioned again later, the adsorbates associated with curve A appear to bond to surface hydroxyls via

the substituent heteroatom, which those of curve B bond through the ring  $\pi$ -electron system. Similar curves are obtained if the

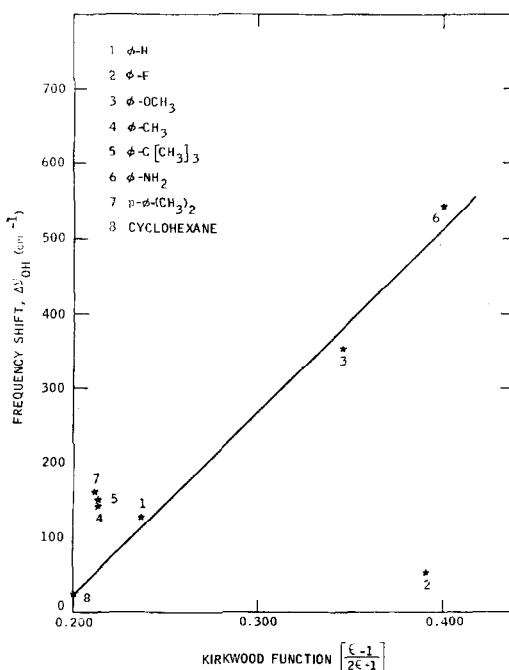


FIG. 2. Frequency shift of the hydroxyl absorption as function of the Kirkwood function, for the room temperature adsorption of various aromatic molecules on porous Vycor glass at a surface coverage of  $\theta = 0.5$ .

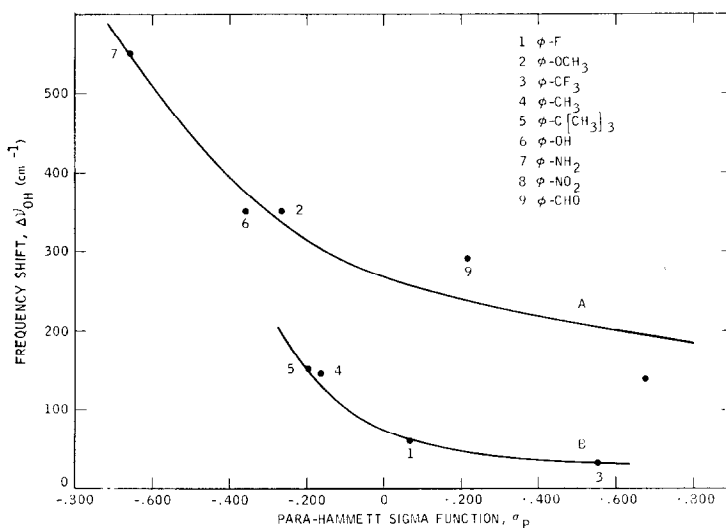


FIG. 3. Frequency shift of the hydroxyl absorption as function of the Hammett sigma function, for the room temperature adsorption of various aromatic molecules on porous Vycor glass at a surface coverage of  $\theta = 0.5$ .

metasubstituent constant is used. Thus it appears that there is a general trend of a decrease in the electron-donating power of a substituent (i.e., more positive  $\sigma$  values) accompanying a decrease in the degree of charge transfer to the aromatic ring and hence a decrease in the strength of the surface bond as reflected by  $\Delta\nu_{\text{OH}}$ . Such results suggest that a charge-transfer model might be useful.

One can postulate for energy contributions to the hydrogen bond: electrostatic interaction, dispersion forces, exchange repulsion, and delocalization energy. The neglect of the last two contributions leads to the failure of the electrostatic theories, the infrequent successes of such models being probably due to the fortuitous algebraic cancellation of those two energy contributions. For example, Tsubomura (12) found proton-accepting strengths to decrease in the order diethyl ether  $\approx$  acetone, acetonitrile, while the electrostatic theory would predict the opposite trend on the basis of group polarity. It was concluded that the delocalization energy for hydrogen bonding increased in the order acetonitrile  $>$  acetone  $>$  diethyl ether, and thus compensated or overwhelmed the increase in electrostatic energy.

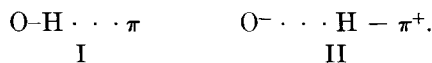
An alternative and more reasonable approach to such systems is the charge-transfer model developed by Mulliken (13-16) for hydrogen bonding in homogeneous systems and later modified by Puranik (17, 18). We have consequently applied their theory to the present heterogeneous systems.

#### The Charge-Transfer Model

Let us assume, as suggested by our prior results (1, 2), that an interaction is established between the aromatic  $\pi$ -orbitals of the adsorbate and the surface hydroxyl groups. The wavefunction for the ground-state-bonded molecule is

$$\psi_c = a\psi_0 + b\psi_1, \quad (1)$$

where  $\psi_0$  and  $\psi_1$  are the wavefunctions associated with the respective resonance structures,



$\psi_0$  and  $\psi_1$ , respectively, refer to the so-called no-bond and dative bond wavefunctions of the Mulliken theory, and  $\pi$  represents participation of the aromatic  $\pi$  orbitals. The first term of Eq. (1) corresponds to the usual forces considered, i.e., dispersion and electrostatic forces as well as the repul-

sion energy which originates from exchange repulsion forces. The novel feature in formulating the wavefunction of the adsorbed complex,  $\psi_c$ , is the second term representing charge-transfer contributions. The term  $b\psi_1$  indicates that an electron has left a non-bonding donor orbital  $\Phi_D$  (a  $\pi$ -orbital from the aromatic nucleus) and entered an antibonding acceptor orbital  $\Phi_A$  (on the surface OH group), thus establishing a somewhat weak covalent bond. (We have assumed the electron to enter an antibonding orbital of the hydroxyl because one observes a weakening of the O-H bond upon interaction with the adsorbing molecule (2) and hence a decrease in bond order.) Then, using a perturbation technique (see the Appendix) one finds the surface-complex energy  $W_c$  to be (in Dirac notation),

$$W_c = \langle \psi_c | \hat{H} | \psi_c \rangle \approx W_0 - (H_{01} - SW_0)^2 / (W_1 - W_0) + \dots, \quad (2-a)$$

$$\text{where } W_0 \equiv \langle \psi_0 | \hat{H} | \psi_0 \rangle, \quad (2-b)$$

$$W_1 \equiv \langle \psi_1 | \hat{H} | \psi_1 \rangle, \quad (2-c)$$

$$H_{01} \equiv \langle \psi_0 | \hat{H} | \psi_1 \rangle, \quad (2-d)$$

$$S \equiv \langle \psi_0 | \psi_1 \rangle. \quad (2-e)$$

As in the Mulliken theory, the complex is stabilized by resonance between the two major contributing structures I and II. The resonance energy in the ground state due to such stabilization (i.e., between  $\psi_0$  and  $\psi_1$ ) is given by,

$$E = W_0 - W_c = (H_{01} - SW_0)^2 / (W_1 - W_0). \quad (3)$$

$E$  will be large if  $(W_1 - W_0)$  is reasonably small and  $(H_{01} - SW_0)^2$  is large enough, which is generally the case when  $\psi_0$  and  $\psi_1$  overlap sufficiently (i.e., large values for  $S$ ) and possess the same symmetry. It can be shown (16) that, if  $\psi_0$  and  $\psi_1$  are not the same group theoretical species,  $H_{01}$  and  $S$  are zero, i.e., no overlap.

The weighting coefficient  $b$  of Eq. (1), a measure of the degree of charge transfer, is (see Eq. A-15)

$$b = cS / (I_D - E_A - W), \quad (4)$$

where  $I_D$  is the donor (adsorbate) ionization potential,  $E_A$  the acceptor (surface OH)

electron affinity, and  $W$  the net coulombic energy of attraction between the negative and positive parts of the charge-transfer complex.

Equation (4) can now be related to the spectroscopic parameters.  $\Delta\nu_{\text{OH}}$  is derived by assuming that the perturbation caused by the adsorbed molecule brings about a decrease in bond order of the hydroxyl through the donation of a mobile electron from the  $\pi$ -system of the adsorbed molecule to an antibonding orbital of the surface hydroxyl. The resulting expression is [see Eq. (B-15)],

$$I_D = [(5/4)^{1/2} cS\lambda^{1/2} (\Delta\nu_{\text{OH}}/\nu_0)^{-1/2} + (E_A + W)], \quad (5)$$

where  $\nu_0$  is the fundamental vibrational frequency of the unperturbed surface hydroxyl ( $3747 \text{ cm}^{-1}$ ),  $\lambda$  is defined by Eq. (B-5) and is a measure of the charge distribution within the O-H bond before adsorption.

Perhaps the most significant observation to be made is that the hydroxyl band shift is quantitatively related to the ionization potential of the adsorbing molecule. Consequently, for the interactions of a series of donor molecules (e.g., aromatics, having similar donor orbitals, so that the overlap integral  $S$  is approximately constant) with a given acceptor orbital (hydroxyls, so that  $\lambda$  is constant), a plot of  $I_D$  versus  $(\Delta\nu_{\text{OH}}/\nu_0)^{-1/2}$ , the Mulliken-Puranik parameter, should be linear. The slope is  $[(5/4)^{1/2} cS\lambda^{1/2}]$ . The intercept on the ordinate gives the value of  $(E_A + W)$ , where  $E_A$  is the electron affinity of the surface hydroxyl group.  $W$  is essentially a coulombic term and a function of the  $\text{O}^- \cdots \pi^+$  distance.

The increase in infrared integrated absorption intensity for the hydroxyl can be derived in a similar fashion (Appendix C). The increase in intensity is attributed predominantly to an increased dipolar character of the group, as suggested by resonance structures such as  $\text{O}^- \cdots \text{H} - \pi^+$ . The expression for the integrated intensity  $A$  is [Eq. (C-7)],

$$A = 10^{-3} (N\pi/3mc^2) \{ 4/5 (\vec{\mu}_p/\lambda) \times [\partial(1/S^2)/\partial r]^2 (\Delta\nu_{\text{OH}}/\nu_0)^2 \} \quad (6)$$

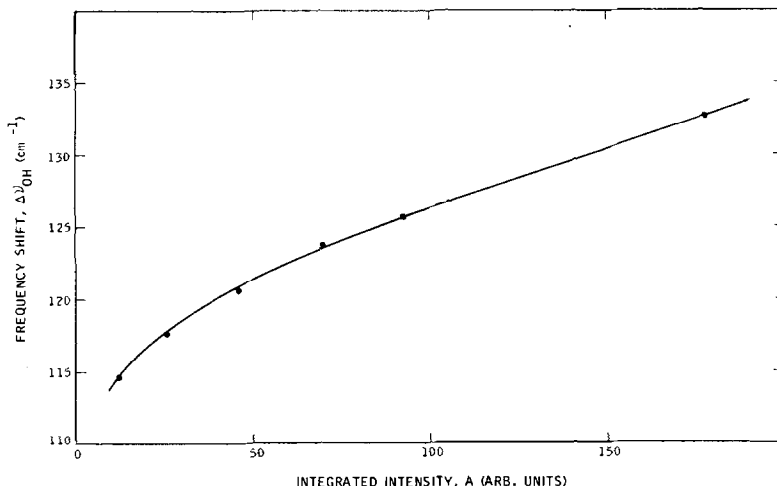


FIG. 4. Benzene adsorption on porous Vycor glass at room temperature.

where  $\vec{\mu}_p$  is the molecular dipole moment associated with the polar resonance structure II and all other terms have their usual meaning. Empirical relationships between the integrated intensity and the corresponding band shifts for the free hydroxyl groups have been found for many systems (19-21), and such a relation exists for benzene adsorption on porous glass, as shown in Fig. 4. However, the present charge-transfer treatment is the first to predict such a relationship with any precision. The relations suggest that the changes in both spectroscopic parameters could have a common cause. Equation (6) provides an easy test for the charge-transfer model in that a plot of  $A^{1/2}$  versus  $\Delta\nu_{OH}/\nu_0$  should be linear if the other terms are constant.

#### DATA ANALYSIS USING THE CHARGE-TRANSFER MODEL

##### *The Hydroxyl Shift, $\Delta\nu_{OH}$*

Figure 5 shows the relations obtained when the shift data for a variety of aromatic adsorbates are considered in terms of Eq. (5). The linearity of the plots is a prime indication of the usefulness of the charge-transfer model in describing the interactions of the aromatics with the surface hydroxyls of porous glass. Significantly, the data fall into three groups, the plots describing the

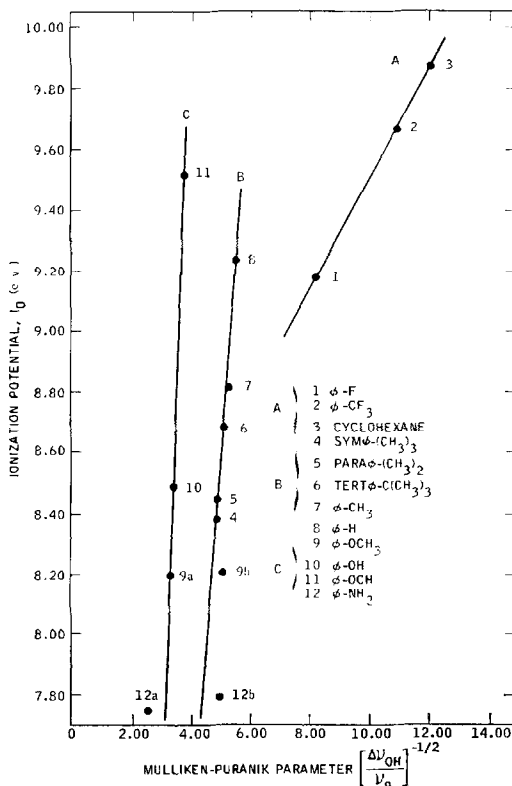


FIG. 5. Application of charge-transfer theory to the hydroxyl frequency shift, for aromatics adsorbed on porous Vycor glass at room temperature at a surface coverage of  $\theta = 0.5$ . Points 9a and 12a refer to the shift produced by the heteroatoms; points 9b and 12b refer to the shift attributed to the  $\pi$ -OH interaction.

behavior of fluoro-, methyl-, and oxysubstituted benzenes.

For the fluoro-aromatics of plot A, assuming the molecules to interact with the surface hydroxyls via the  $\pi$ -electron systems, an increasing degree of electron delocalization towards the fluorine atoms is observed, so that there is a decrease in interaction energy, i.e., an increase in  $(\Delta\nu_{\text{OH}}/\nu_0)^{-1/2}$ , until the energy approaches that of a saturated ring. The interaction decreases in the order  $\phi\text{F} > \phi\text{-CF}_3 > \text{C}_6\text{H}_{12}$ . If the adsorption were to occur via the fluorine substituents, then  $\phi\text{-CF}_3$  would be more strongly bound than  $\phi\text{F}$  because of the greater electron density about the fluorine atoms.

Analogous arguments apply to plot B. There would be a progressive electron enrichment of the  $\pi$  orbitals of adsorbates with increasing donor strength of the ring substituents. As methyl groups are good electron donors, there would be an increase in the interaction energy on going from benzene to mesitylene. The energy changes in the order shown by plot B.

For the aromatics of plot C, the strong adsorption does not occur primarily through the  $\pi$ -electron system. This view is based on the fact that the hetero groups involved,  $-\text{OCH}_3$ ,  $-\text{OH}$ ,  $-\text{OCH}$ , and  $-\text{NH}_2$ , are all very strong adsorption agents even when attached to relatively unreactive alkyl chains (7). Also, ultraviolet spectroscopic studies (22-25) indicate that phenol and aniline adsorb via their substituent groups on silica. However, aniline and anisole are special cases.

Recent experiments (26) on the adsorption of aniline on porous glass and on silica showed that an intense, broad perturbed hydroxyl band with  $\Delta\nu_{\text{OH}} = 550 \text{ cm}^{-1}$  was produced, and also a much weaker band with  $\Delta\nu_{\text{OH}} = 150 \text{ cm}^{-1}$ . In keeping with others (7), the intense band was attributed to bonding to OH through the nitrogen atom. The weaker band was attributed to a  $\pi$ -OH interaction. Aniline is thus taken to interact with hydroxyls principally through its heteroatom, with a quite small contribution to the bonding due to the ring-OH interaction (26). A much more pronounced dual interaction was reported for anisole

(27). Two fairly strong perturbed hydroxyl bands with  $\Delta\nu_{\text{OH}}$  of  $350 \text{ cm}^{-1}$  and  $150 \text{ cm}^{-1}$  were observed. Various data suggested that the adsorbed aniline could be doubly bonded to surface hydroxyls by simultaneous interactions via the nitrogen atom as well as the benzene ring. Two  $\Delta\nu_{\text{OH}}$  values corresponding to the heteroatom-OH and  $\pi$ -OH interactions of aniline and anisole are given in Table 1 and Fig. 5. The  $\Delta\nu_{\text{OH}}$  values for the  $\pi$ -OH interaction of both compounds fall near plot B of Fig. 5, but in view of the excellent agreement of data points 4 through 8 of plot B, the two values of 9b and 12b actually fall fairly far off the plot. However, as plot B reflects the "activity" of electron-rich rings, while the rings of aniline and anisole would be somewhat electron-depleted, the deviation of the two points is not significant.

The slopes of the plots of Fig. 5 may be considered in terms of the variable  $S$ , the overlap integral, and  $\lambda$ , the bond polarity parameter [see Eq. (5)]. The degree of separation of the data into three distinct plots is a function of  $S$  and  $\lambda$ . For example, the oxysubstituted aromatics of plot C, Fig. 5, form bonds through similar orbitals, while the  $sp^3$  lone-pair of the nitrogen atom is involved in the case of aniline. As the overlap integral of the latter is greater than that for the oxygen bonding, it is not surprising that aniline shows deviations with respect to the data of plot C. However, both the fluorine- and methyl-substituted aromatics of plots A and B bond via their  $\pi$ -orbitals, and it is difficult to explain why the data fall into two sets. Possibly, fluorine substitution causes such drastic electron drainage that the overlap integral  $S$  is affected significantly.

As far as molecular orbitals are concerned, three reasonable models may be considered (Fig. 6), as in the case of some homogeneous hydrogen bonding systems (28). The hydroxyl proton could be located on the axis of symmetry perpendicular to the plane of the benzene ring (Fig. 6A). In that case, the overlap integral, involving the highest occupied  $\pi$ -orbital ( $e_{2g}$ ) of the ring from which the electron is assumed to be donated and also the hydroxyl anti-



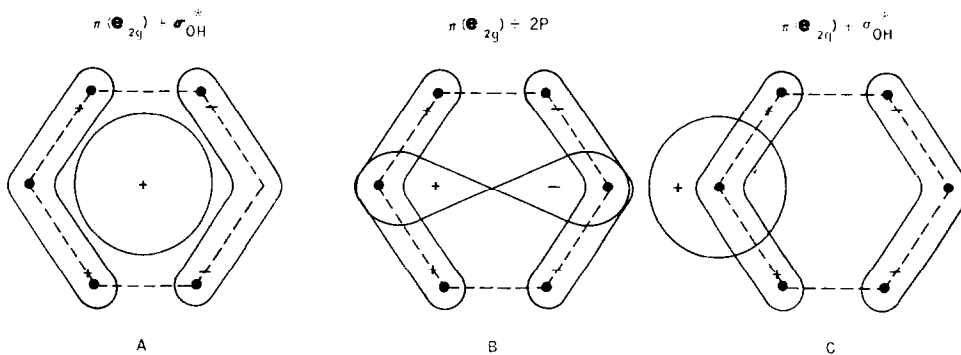


Fig. 6. Possible molecular orbitals for the geometry of a surface aromatic-hydroxyl bond.

bonding orbital  $\sigma_{OH}^*$ , is zero for symmetry reasons. The second structure B is discarded because of the high promotional energy of the  $2p$  orbital of the hydrogen atom. The third structure is the most reasonable because it is a lower energy structure and gives rise to maximum overlap. In that configuration the hydrogen atom occupies a position on the axis perpendicular to the ring and passing through a carbon atom or through the center of a C-C bond, a "ring current" region.

For the adsorbates of plot C of Fig. 5, adsorption most likely occurs via the non-bonding electrons on the heteroatoms (oxygen and nitrogen). The bonding strength of

anisole in comparison to that of phenol or benzaldehyde is reasonable, because the methyl group is a good electron donor and would be expected to increase the degree of charge-transfer through the oxygen  $p$  orbitals of the anisole. The large deviation of aniline is explainable in terms of  $sp^3$  hybridization of its nitrogen atom. Bonding of the surface hydroxyl by use of the unpaired electrons on the nitrogen (in an  $sp^3$  orbital) involves a higher degree of orbital overlap than that for the  $p$  orbitals of oxygen. Such is usually the case for hybridized versus unhybridized overlap. Thus Cannon found (8) that when all other variables were held constant, the degree of

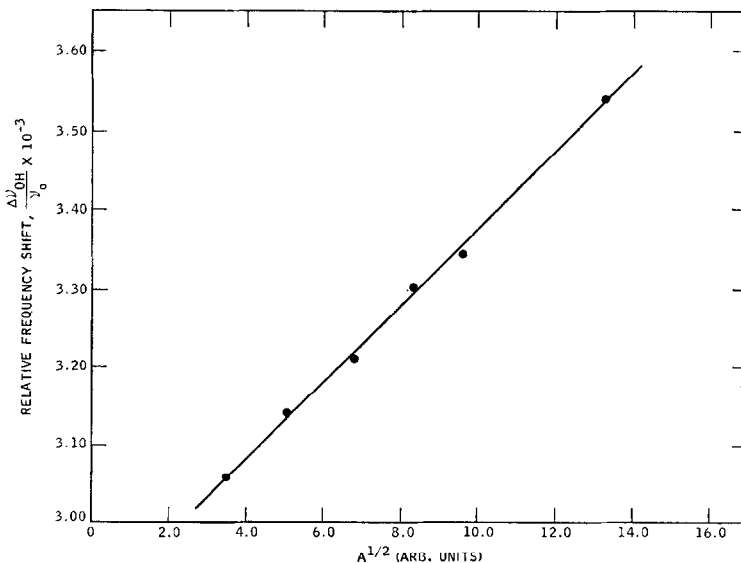


Fig. 7. Application of charge-transfer theory to the hydroxyl band intensity, for benzene adsorbed on porous Vycor glass at room temperature.

overlap and hence interaction for a hydrogen bonding system increased in the order  $sp^3 > sp^2 > sp > p$ . The increased overlap gives a higher value for the overlap integral  $S$  and thus a greater degree of interaction. The differences in  $\Delta\nu_{OH}$  values of anisole, aniline, and benzaldehyde are not surprising. From Table 2 it is apparent that, in general, the oxygen atoms of ethers are much more reactive electron donors than carbonyl oxygen atoms for the same interaction with surface hydroxyls. Apparently, for two adsorbates of the general structures R-O-R'

and  $\text{R}-\overset{\text{O}}{\parallel}\text{C}-\text{R}$ , the former is the better electron donor. This is due to the fact that the unpaired electrons on the ether oxygen are in  $sp^3$  orbitals whereas those on the ketone oxygen are in  $s$  and  $p$  orbitals. Thus one observes stronger hydrogen bond formation in the case of ethers because of the greater degree of orbital overlap.

#### Band Intensity Enhancement

A set of band intensity data is available only for the adsorption of benzene on porous glass. As indicated by Eq. (6), a plot of  $\Delta\nu_{OH}/\nu_0$  versus  $A^{1/2}$  should be linear. Such data are shown in Fig. 7. The linearity of the plots indicates that the theory "fits" well.

#### General Data Correlation

The success of the charge-transfer model in treating different types of adsorbates is shown by the plots of Fig. 8. Each of the plots A to G relates the behavior of similar adsorbate molecules. For these, there are five anomalies. The latter include aniline (No. 6) and anisole (No. 37), which have already been discussed.

Furan (No. 15) has been found to bond only through the  $\pi$ -system and not through the oxygen atom (19), as with other ether-like adsorbates; a great deal of the electron density of the oxygen is delocalized to the ring. The behavior of the other three adsorbates is probably due to similar effects, because in each case there is a significant extent of charge delocalization from the heteroatom to the ring. Under such circum-

stances, values for parameters such as  $S$  and  $\lambda$ , which were considered to be constant in Eq. (5) for a given group of similar adsorbents, would change their values.

Figure 8 also shows some data for a few unrelated adsorbents. Not enough data are available to consider these in detail.

In general it appears that the charge-transfer model is an extremely useful one. More infrared work on the adsorption of series of similar molecules on hydroxyls bound to different solid surfaces will be carried out. Additional pertinent information could come from careful measurements of electronic spectra of molecules adsorbed on carefully degassed hydroxylated surfaces. Such data do not seem to be available; the data in the literature pertain to materials adsorbed from the liquid state onto poorly prepared surfaces. Of course, a charge-transfer interaction does not necessarily imply the formation of ion pairs. The theory is valid even for the weakest interactions,

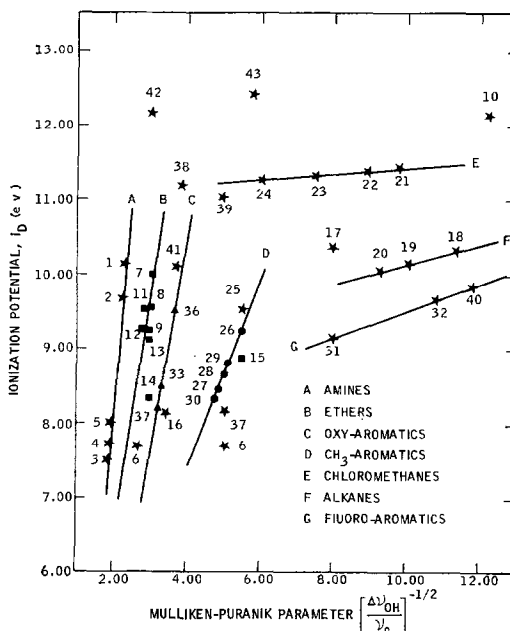


Fig. 8. Application of charge-transfer theory to the hydroxyl frequency shift, for a variety of molecules interacting with hydroxyls at room temperature at a surface coverage of  $\theta = 0.5$ . The numbers identifying the data points and compounds correspond to those given in the first columns of Tables 1 and 2.

e.g., fluorobenzene adsorbed on porous glass, if the assumptions which were made are valid. A strong charge-transfer band may not be observed for such weakly interacting systems, the intensity of the transition band being determined by the value of  $b$  in Eq. (1).

#### ACKNOWLEDGMENT

Support by means of a Grant from the National Air Pollution Control Administration is gratefully acknowledged.

#### APPENDIX

##### A. Derivation of the Surface-Complex Energy

$$\hat{H}\psi_c = W_c\psi_c, \quad (\text{A-1})$$

$$\hat{H}(a\psi_0 + b\psi_1) = W_c(a\psi_0 + b\psi_1), \quad (\text{A-2})$$

where  $\hat{H}$  is the exact Hamiltonian operator for the entire set of nuclei and electrons. Next one multiplies Eq. (A-2) by  $\psi_0$  and integrates over all space to get

$$aW_0 + bH_{01} = aW_c + bW_cS. \quad (\text{A-3})$$

Performing the same operation again with  $\psi_1$  gives

$$aH_{10} + bW_1 = aW_cS + bW_c. \quad (\text{A-4})$$

(A-3) and (A-4) form a set of simultaneous equations in two unknowns:

$$\begin{cases} (H_{01} - W_cS)a + (W_1 - W_c)b = 0 \\ (W_0 - W_c)a + (H_{01} - W_cS)b = 0 \end{cases} \quad (\text{A-5})$$

in which  $H_{10}$  has been replaced by  $H_{01}$  because of the Hermitian property of that operator. Then for a nontrivial solution of (A-5)

$$\left| \begin{array}{cc} (H_{01} - W_cS)(W_1 - W_c) \\ (W_0 - W_c)(H_{01} - W_cS) \end{array} \right| = 0 \quad (\text{A-6})$$

or

$$W_c = W_0 - \frac{(H_{01} - W_cS)^2}{(W_1 - W_c)}. \quad (\text{A-7})$$

For the second term on the right side of (A-7) one makes the approximation that  $W_c \approx W_0$ . This simply means that in the ground state there is only a small degree of charge-transfer character for the surface

complex, and  $\psi_0$  makes a more significant contribution than  $\psi_1$ . Thus,

$$W_c = W_0 - \frac{(H_{01} - W_cS)^2}{(W_1 - W_0)}. \quad (\text{A-8})$$

In (A-8),  $W_c$  is the ground-state energy of the surface charge-transfer complex;  $W_0$  is equal to the sum of any energy of repulsion or attraction arising from ionic, ion-dipole, dipole-dipole, dispersion, or polarization forces; and  $W_1$  has a similar meaning as  $W_0$ , but also includes the attractive energy due to ionic and covalent bonding.

The weighing coefficients  $a$  and  $b$  in Eq. (A-2) are readily obtained from Eq. (A-6). Thus

$$b/a = -\frac{(H_{01} - W_0)}{W - W_0}, \quad (\text{A-9})$$

where again we have replaced  $W_c$  by  $W_0$  in the denominator of (A-9).

One can now solve for  $b$ , which is proportional to the degree of charge transfer. Following Puranik (17) we assume the integral  $H_{01}$  to be proportional to the overlap integral  $S_{DA}$  for the donor molecular orbital  $\Phi_D$  (aromatic  $\pi$ -system) with that of the acceptor orbital (surface free OH group); i.e.,

$$H_{01} \equiv \langle \psi_0 | \hat{H} | \psi_1 \rangle \propto S_{DA} = \langle \Phi_D | \Phi_A \rangle. \quad (\text{A-10})$$

In addition, one assumes  $S_{AB} \propto S$  (16), where  $S$  is given by Eq. (2-e). Thus  $H_{01} = c'S$  where  $c'$  is a constant. Then from (A-9)

$$\begin{aligned} b/a &= -(H_{01} - SW_0)/(W_1 - W_0) \\ &= -(H_{01} - SW_0)/\Delta W \\ &= S(W_0 - c')/\Delta W = cS/\Delta W, \end{aligned} \quad (\text{A-11})$$

where  $c$  is also a constant. From the normalization requirement,

$$\langle \psi_c | \psi_c \rangle = 1 \quad (\text{A-12})$$

one calculates that  $a^2 + abS + b^2 = 1$ . Then substitution of  $a = \Delta Wb/cS$  into this expression gives

$$b^2(\Delta W^2/c^2S + 2\Delta W + 1) = 1. \quad (\text{A-13})$$

However,  $\Delta W \gg S$ , so that  $(2\Delta W + 1) \ll \Delta W^2/c^2S$  and thus one gets

$$b \cong cS/\Delta W = cS/(W_1 - W_0). \quad (\text{A-14})$$

$(W_1 - W_0)$  can then be replaced by  $(I_D -$

$E_A - W$ ), where  $I_D$  is the first ionization potential of the donor molecule,  $E_A$  is the electron affinity of the acceptor molecule, and  $W$  is the net coulombic energy of attraction between the negative and positive parts of the surface charge-transfer complex. Therefore,

$$b = cS/(I_D - E_A - W). \quad (\text{A-15})$$

From (A-15) it is apparent that  $b$ , which is a measure of the degree of charge transfer, increases with increasing overlap and electron affinity, but decreases with increasing donor ionization potential. These are properties which one would expect for a charge-transfer process.

### B. The Free-Hydroxyl Frequency Shift

The molecular orbital for the mobile or delocalized electron is given by

$$\Phi = c_1\Phi_A + c_2\Phi_D, \quad (\text{B-1})$$

where  $\Phi_A$  is the antibonding acceptor orbital of the OH group and  $\Phi_D$  is the nonbonding donor orbital (aromatic  $\pi$ -orbital).  $c_1$  and  $c_2$  are related to the probability of finding the electron in the molecular orbitals  $\Phi_A$  and  $\Phi_D$ , respectively. The probability of finding an electron in  $\Phi_A$  is the same as the probability of charge transfer. Thus one can replace  $c_1$  by  $b$  and  $c_2$  by  $a$ .

$$\Phi = b\Phi_A + a\Phi_D, \quad (\text{B-2})$$

where  $b$  and  $a$  are related by (A-9).

In the LCAO-MO approximation, assuming the complex to be a heteronuclear diatomic group, the antibonding acceptor orbital is given (35) by

$$\Phi_A = \phi_1 - \phi_2, \quad (\text{B-3})$$

where  $\phi_1$  and  $\phi_2$  are the pertinent atomic orbitals of the surface OH group, and  $\lambda$  is a mixing coefficient which is a measure of the polarity of the orbitals.  $\lambda$  is readily related to the molecular dipole moment by

$$\overline{\mu}_{NM} = -e\langle\phi_N \left| \sum_i r_i \right| \phi_M\rangle \quad (\text{B-4})$$

from which (36)

$$\overline{\mu} = [(\lambda^2 - 1)eR]/(1 - \lambda^2 + 2\lambda S) \quad (\text{B-5})$$

then from (B-3) and (B-2)

$$\Phi = b(\phi_1 - \lambda\phi_2) + a\Phi_D, \quad (\text{B-6})$$

where  $\Phi$  is the molecular orbital for the mobile or delocalized electron involved in the formation of the surface charge-transfer complex.

The contribution of this mobile electron to the O-H bond order is given by a relationship derived by Coulson (37); viz.,

$$p = b^2\lambda, \quad (\text{B-7})$$

where  $p$  is the bond order and  $\lambda$  is given by Eq. (B-5). After the surface charge-transfer complex is formed, the total bond order of the OH group is

$$1 - p = 1 - b^2\lambda. \quad (\text{B-8})$$

Using Gordy's relationship which connects force constants, bond order and bond length,

$$k_m/k_n = (p_m/p_n)(d_n/d_m)^{3/2}, \quad (\text{B-9})$$

and also approximating the surface complex by a diatomic oscillator, one gets

$$(\nu_1/\nu_2)^2 = (p_1/p_2)(d_2/d_1)^{3/2}, \quad (\text{B-10})$$

where  $\nu_1$ ,  $\nu_2$ ;  $p_1$ ,  $p_2$ ;  $d_1$ ,  $d_2$  are, respectively, the frequencies, bond orders, and bond lengths before and after complex formation for the surface OH group. Now, assuming that bond lengths are inversely proportional to bond orders (17, 18) gives,

$$\nu_1/\nu_2 = (p_1/p_2)^{5/4}. \quad (\text{B-11})$$

However, the bond order before complex formation ( $p_1$ ) is unity, and after complex formation is  $(1 - p)$ . Therefore, Eq. (B-11) can be rewritten as,

$$\nu_2/\nu_1 = (1 - p)^{5/4}. \quad (\text{B-12})$$

The right side of Eq. (B-12) can be expanded by the Binomial Theorem, and neglecting higher powers of  $p$  and combining with (B-7) gives,

$$(\nu_2 - \nu_1)/\nu_1 = \Delta\nu/\nu_1 = 5/4(b^2\lambda). \quad (\text{B-13})$$

Substituting for  $b$  in (B-13) from Eq. (A-15) gives the final result for the frequency shift of the free hydroxyl band; i.e.,

$$\Delta\nu_{\text{OH}}/\nu_0 = (5/4)\lambda c^2 S^2 / (I_D - E_A - W)^2 \quad (\text{B-14})$$

which may be recast into

$$I_D = [(5/4)^{1/2}cS\lambda^{1/2}](\Delta\nu_{OH}/\nu_0)^{-1/2} + (E_A + W). \quad (\text{B-15})$$

### C. Intensity Changes

Integrated intensity enhancements may be attributed to increased dipolar character as suggested by resonance structures such as  $O^- \cdots H - \pi^+$ , for which the contribution to the total dipole moment due to this structure is given by

$$\overrightarrow{\mu_T} = \overrightarrow{\mu_p} b^2. \quad (\text{C-1})$$

Here  $b^2$  is a weighing coefficient, and is a relative measure of the contribution of the ionic structure to the total moment while  $\overrightarrow{\mu_p}$  is the dipole moment associated with this resonance structure, and is given roughly by the product of the electronic charge and the  $O^- - \pi^+$  bond distance  $eR$ . We have neglected the contribution from  $OH \cdots \pi$ , because it will be very much less than that from the ionic structure. One then calculates that

$$\overrightarrow{\partial\mu_T}/\partial r = \overrightarrow{\mu_p}(\partial b^2/\partial r) \quad (\text{C-2})$$

where we have assumed that  $\overrightarrow{\mu_p} \neq f(r)$  which is true for not too strongly bound species.

Combining Eqs. (A-15) and (C-2) gives

$$\overrightarrow{\partial\mu_T}/\partial r = [\overrightarrow{\mu_p}c^2/(I_D - E_A - W)^2](\partial S^2/\partial r) \quad (\text{C-3})$$

which arranges to

$$I_D = c[\overrightarrow{\mu_p}(\partial S^2/\partial r)]^{1/2}(\overrightarrow{\partial\mu_T}/\partial r)^{-1/2} + (E_A + W). \quad (\text{C-4})$$

Then for a given acceptor molecule and a series of donor molecules containing the same donor orbitals, a plot of  $I_D$  versus  $(\overrightarrow{\partial\mu_T}/\partial r)^{-1/2}$  should be linear. A relationship between the integrated intensity and band shift can be deduced by equating the right-hand sides of Eqs. (C-4) and (B-15), so that

$$\overrightarrow{\partial\mu_T}/\partial r = -(4/5)(\overrightarrow{\mu_p}/\lambda)[\partial(1/S^2)/\partial r] \times (\Delta\nu_{OH}/\nu_0). \quad (\text{C-5})$$

The integrated absorption intensity is given by

$$A = 10^{-3}(N\pi/3mc^2)(\overrightarrow{\partial\mu_T}/\partial r)^2 \quad (\text{C-6})$$

(in the harmonic oscillator approximation); on combining (C-6) and (C-5) one gets

$$A = 10^3(N\pi/3mc^2)\{(4/5)(\overrightarrow{\mu_p}/\lambda) \times [\partial(1/S^2)/\partial r]\}^2(\Delta\nu_{OH}/\nu_0)^2. \quad (\text{C-7})$$

### REFERENCES

1. CUSUMANO, J. A., AND LOW, M. J. D., *J. Phys. Chem.* **74**, 792 (1970).
2. CUSUMANO, J. A., AND LOW, M. J. D., *J. Phys. Chem.* **74**, 1950 (1970).
3. McDONALD, J. J., *J. Amer. Chem. Soc.* **79**, 850 (1957).
4. FOLMAN, M., AND YATES, D. J. C., *Proc. Roy. Soc. Ser. A* **246**, 32 (1958).
5. FOLMAN, M., AND YATES, D. J. C., *Trans. Faraday Soc.* **54**, 429, 1684 (1958).
6. PIMENTAL, G. C., AND MCCLELLAN, A. L., "The Hydrogen Bond," W. H. Freeman & Co., San Francisco, 1960.
7. LITTLE, L. H., "Infrared Spectra of Adsorbed Species," Academic Press, New York, 1966.
8. CANNON, C. G., *Spectrochim. Acta* **10**, 341 (1957).
9. WEST, W., AND EDWARDS, R. J., *J. Phys. Chem.* **5**, 14 (1937).
10. BAUER, E., AND MAGAT, M., *J. Phys. (Paris)* **9**, 319 (1938).
11. HAMMETT, L. P., *Chem. Rev.* **17**, 125 (1935).
12. TSUBOMURA, H., *Bull. Chem. Soc. Jap.* **27**, 445 (1954).
13. MULLIKEN, R., *J. Phys. Chem.* **56**, 801 (1952).
14. MULLIKEN, R., *J. Chem. Phys.* **61**, 20 (1964).
15. MULLIKEN, R., *J. Amer. Chem. Soc.* **72**, 600 (1950).
16. MULLIKEN, R., *J. Amer. Chem. Soc.* **74**, 811 (1952).
17. PURANIK, P. G., AND KUMAR, V., *Proc. Indian Acad. Sci. Sect. A* **58**, 29 (1963).
18. PURANIK, P. G., AND KUMAR, V., *Proc. Indian Acad. Sci. Sect. A* **58**, 327 (1963).
19. TSUBUMURA, H., *J. Chem. Phys.* **24**, 927 (1956).
20. HIGGINS, C. M., AND PIMENTAL, G. C., *J. Phys. Chem.* **60**, 1615 (1956).
21. TSUBUMURA, H., *J. Chem. Phys.* **14**, 305 (1946).
22. TSUBUMURA, H., *Nippon Kagaku Zasshi* **82**, 8, 1115 (1961); *J. Chem. Phys.* **24**, 927 (1956).
23. LUTSKII, A. E., AND SHERMET'VA, G. I., *Russ. J. Phys. Chem.* **41**, 403 (1967).
24. ROBIN, M., *J. Chem. Educ.* **33**, 526 (1956).
25. LEERMAKERS, P. A., THOMAS, H. T., WEISS, L. D., AND JAMES, F. C., *J. Amer. Chem. Soc.* **88**, 5075 (1966).

26. LOW, M. J. D., AND SUBBA RAO, V. V., *Can. J. Chem.* **47**, 1281 (1969).
27. LOW, M. J. D., AND CUSUMANO, J. A., *Can. J. Chem.* **47**, 3906 (1969).
28. SZCZEPANIAK, K., AND TRAINER, A., *J. Phys. Chem.* **71**, 3035 (1967).
29. WATANABE, K., NAKAYAMA, T., AND MOTTL, J., *J. Quant. Spectrosc. Radiat. Transfer* **2**, 369 (1962).
30. LOW, M. J. D., RAMASUBRAMANIAN, N., AND SUBBA RAO, V. V., *J. Phys. Chem.* **71**, 1726 (1967).
31. LOW, M. J. D., AND SUBBA RAO, V. V., *Can. J. Chem.* **46**, 3255 (1958).
32. HERTL, W., AND HAIR, M. L., *J. Phys. Chem.* **72**, 4676 (1968).
33. LOW, M. J. D., AND BARTNER, P. L., *Can. J. Chem.* **48**, 7 (1970).
34. LOW, M. J. D., AND SUBBA RAO, V. V., unpublished data.
35. BALHAUSEN, C. T., AND GRAY, H. B., "Molecular Orbital Theory," W. A. Benjamin Inc., New York, 1965, p. 38.
36. COULSON, C. A., "Valence," Oxford University Press, Oxford, 1958, pp. 103ff.
37. COULSON, C. A., *Proc. Roy. Soc. (London)* **169**, 413 (1939).
38. SMYTH, C. P., "Dielectric Behavior and Structure," McGraw Hill, 1955.
39. HINE, J. S., "Physical Organic Chemistry," 2nd Ed., McGraw-Hill, N. Y., 1962.